





Relief of tumor hypoxia using a nanoenzyme amplifies NIR-II photoacoustic-guided photothermal therapy: supplement

QIANG XUE,^{1,2,†} SILUE ZENG,^{2,3,†} YAGUANG REN,^{2,†} YINGYING PAN,^{2,4,†} JIANHAI CHEN,² NINGBO CHEN,^{2,5}  KENNETH K. Y. WONG,⁵  LIANG SONG,² CHIHUA FANG,³ JINHAN GUO,¹ JINFENG XU,¹ CHENGBO LIU,²  JIE ZENG,⁴ LITAO SUN,^{6,7} HAI ZHANG,^{1,8} AND JINGQIN CHEN^{2,9}, 

¹Department of Ultrasound, Shenzhen People's Hospital, The Second Clinical College of Jinan University, The First Affiliated Hospital of Southern University of Science and Technology, Shenzhen 518020, China

²Research Center for Biomedical Optics and Molecular Imaging, Key Laboratory of Biomedical Imaging Science and System, Shenzhen Institute of Advanced Technology, Chinese Academy of Sciences, Shenzhen 518055, China

³Department of Hepatobiliary Surgery, Zhujiang Hospital, Southern Medical University, Guangzhou 510280, China

⁴Department of Medical Ultrasonics, Third Affiliated Hospital of Sun Yat-Sen University, Guangzhou, China

⁵The University of Hong Kong, Department of Electrical and Electronic Engineering, Hong Kong, China

⁶Cancer Center, Department of Ultrasound Medicine, Zhejiang Provincial People's Hospital, Affiliated People's Hospital of Hangzhou Medical College, Hangzhou 310014, China

⁷litaosun1971@sina.com

⁸szzhhans.scc.jnu@foxmail.com

⁹jq.chen@siat.ac.cn

[†]These authors contributed equally

This supplement published with Optica Publishing Group on 6 December 2023 by The Authors under the terms of the [Creative Commons Attribution 4.0 License](https://creativecommons.org/licenses/by/4.0/) in the format provided by the authors and unedited. Further distribution of this work must maintain attribution to the author(s) and the published article's title, journal citation, and DOI.

Supplement DOI: <https://doi.org/10.6084/m9.figshare.24658914>

Parent Article DOI: <https://doi.org/10.1364/BOE.499286>

Relief of Tumor Hypoxia Using a Nanoenzyme Amplifies NIR-II Photoacoustic-Guided Photothermal Therapy

QIANG XUE,^{1,2,†} SILUE ZENG,^{2,3,†} YAGUANG REN,^{2,†} YINGYING PAN,^{2,4,†} JIANHAI CHEN,² NINGBO CHEN,^{2,5} KENNETH K. Y. WONG,⁵ LIANG SONG,² CHIHUA FANG,³ JINHAN GUO,¹ JINFENG XU,¹ CHENGBO LIU,² JIE ZENG,⁴ LITAO SUN,^{6,7} HAI ZHANG,^{1,8} AND JINGQIN CHEN^{2,9}

¹Department of Ultrasound, Shenzhen People's Hospital, The Second Clinical College of Jinan University, The First Affiliated Hospital of Southern University of Science and Technology, Shenzhen 518020, China.

²Research Center for Biomedical Optics and Molecular Imaging, Key Laboratory of Biomedical Imaging Science and System, Shenzhen Institute of Advanced Technology, Chinese Academy of Sciences, Shenzhen 518055, China.

³Department of Hepatobiliary Surgery, Zhujiang Hospital, Southern Medical University, Guangzhou 510280, China.

⁴Department of Medical Ultrasonics, Third Affiliated Hospital of Sun Yat-Sen University, Guangzhou, China.

⁵The University of Hong Kong, Department of Electrical and Electronic Engineering, Hong Kong, China.

⁶Cancer Center, Department of Ultrasound Medicine, Zhejiang Provincial People's Hospital, Affiliated People's Hospital of Hangzhou Medical College, Hangzhou 310014, China.

⁷litaosun1971@sina.com

⁸szzhhans.scc.jnu@foxmail.com

⁹jq.chen@siat.ac.cn

[†]Contributed equally

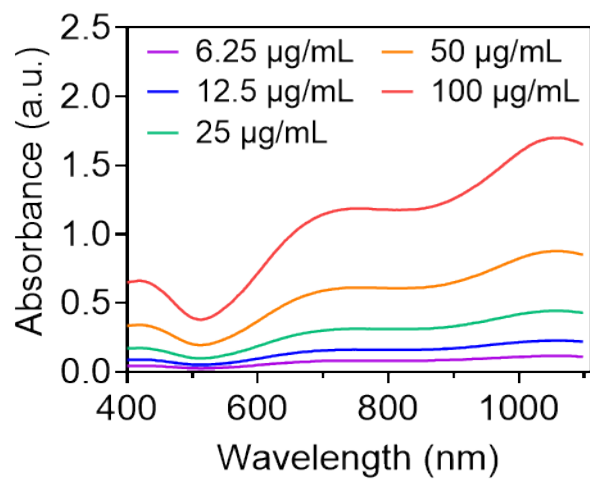


Figure S1. UV-vis-NIR spectra of SPI nanoparticles with different concentrations (6.25, 12.5, 25, 50 and 100 $\mu\text{g/mL}$).

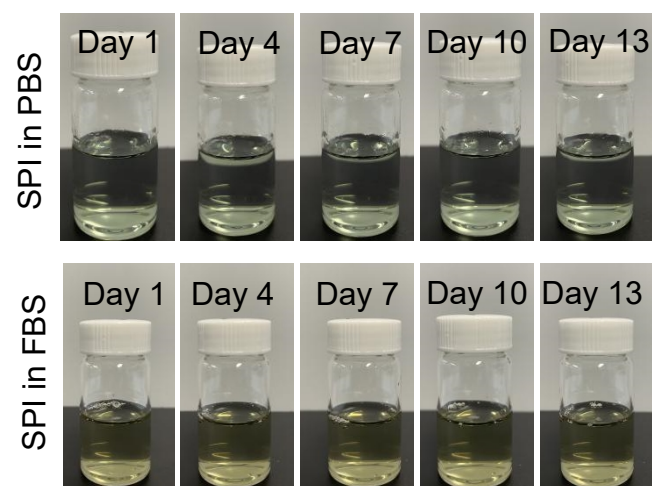


Figure S2. SPI solution photograph in PBS (pH = 7.4) and in FBS (20%) at various time.

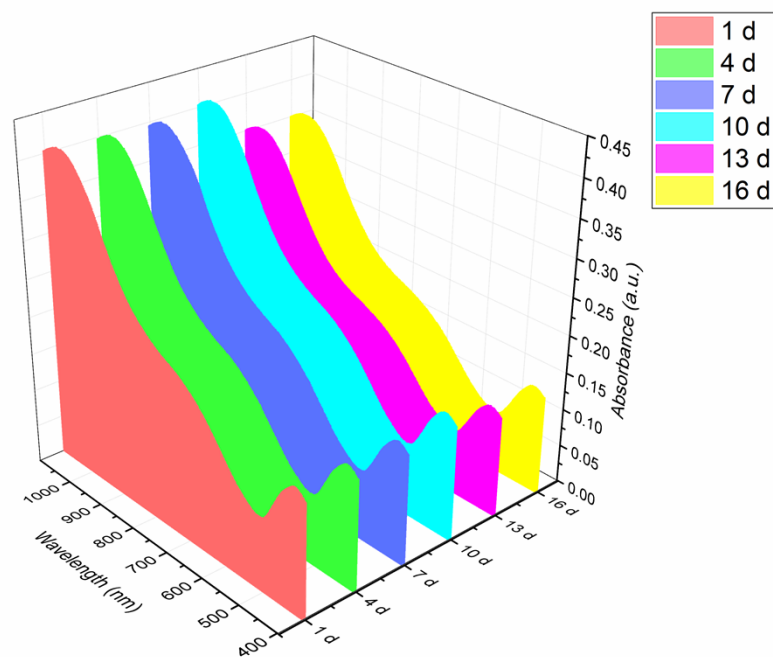


Figure S3. UV-vis-NIR spectra of SPI solution in PBS (pH = 7.4) at various time.

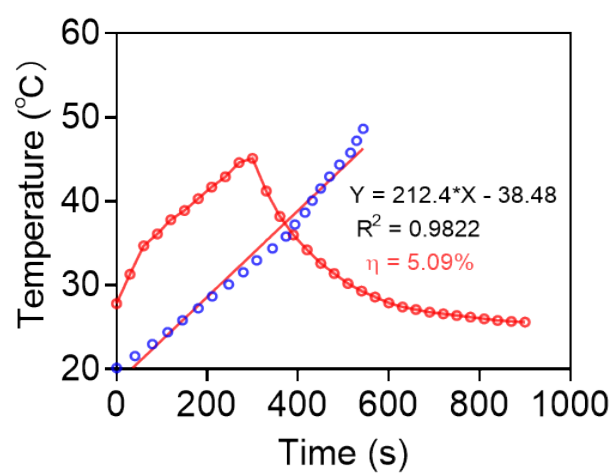


Figure S4. Plot of cooling time of IR1061 solution versus the negative natural logarithm of the temperature driving force obtained from the cooling state, and the corresponding linear fitting curve.

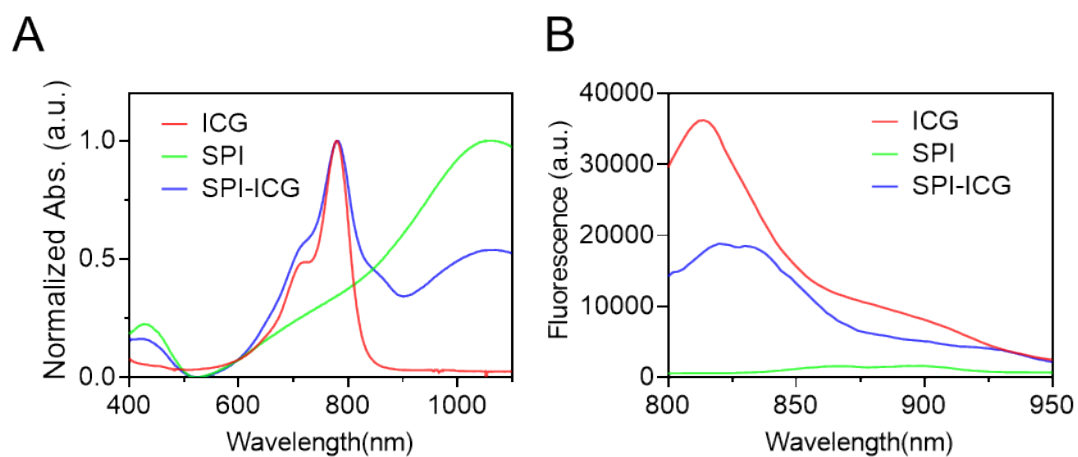


Figure S5. (A) UV-vis-NIR spectroscopy of ICG, SPI and SPI-ICG. (B) Fluorescence spectra of ICG, SPI and SPI-ICG. Excitation = 785 nm.

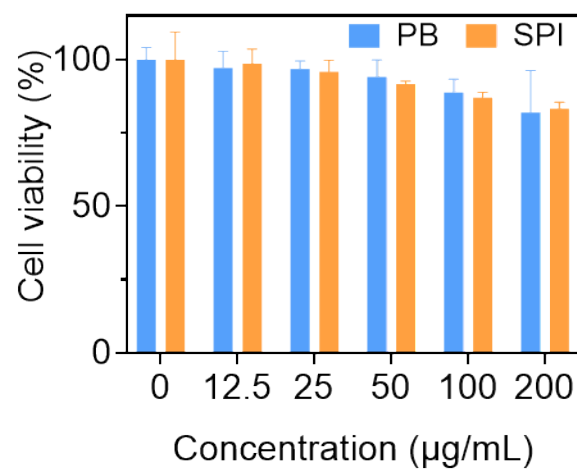


Figure S6. Viability of HUVEC cells treated with different concentrations of PB and SPI.

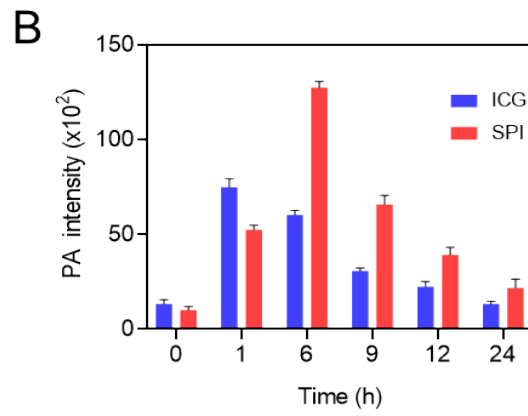
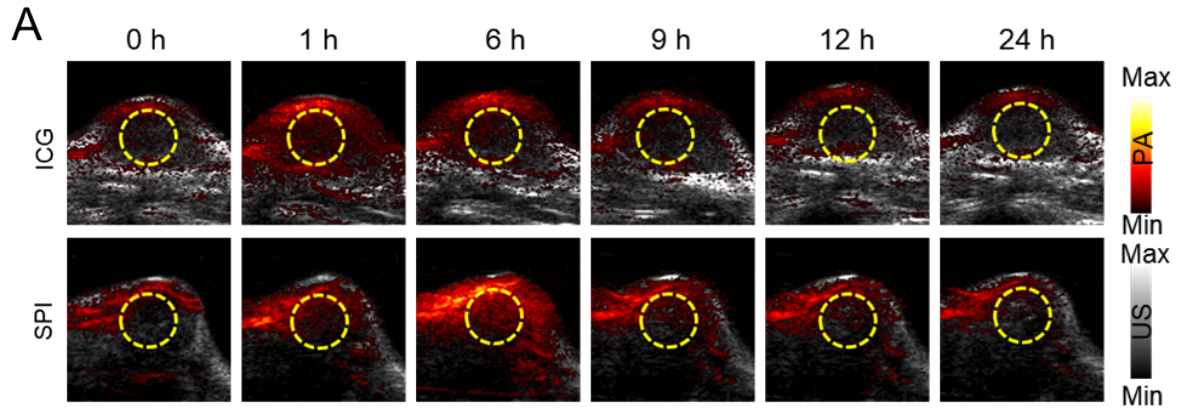


Figure S7. (A) In vivo PA images and (B) quantification results of subcutaneous 4T1 tumor-bearing mice at different time points after intravenous injection of SPI and ICG, respectively.

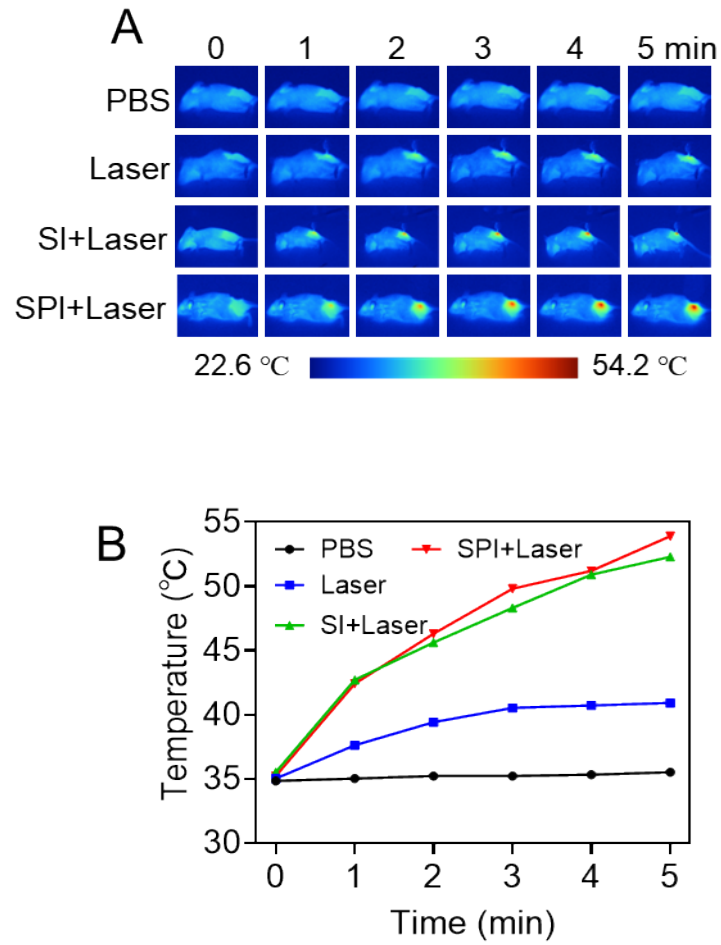


Figure S8. (A) Infrared thermal images and (B) The change in tumor temperature of subcutaneous 4T1 tumor-bearing mice after treatment of PBS, Laser, SI+Lasr, SPI+Laser.

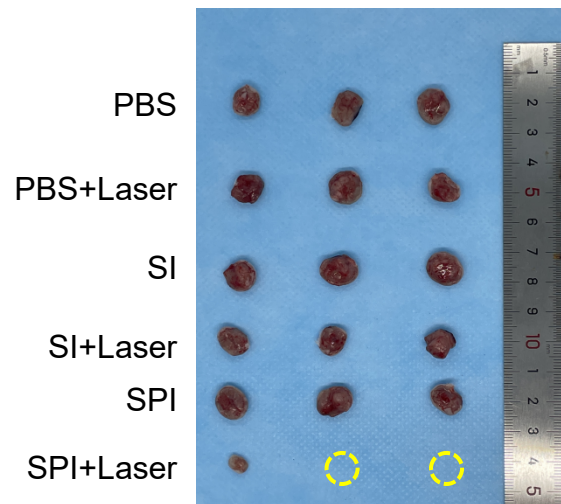


Figure S9. Photograph of excised tumors from six different groups at the end of 14 days treatment.

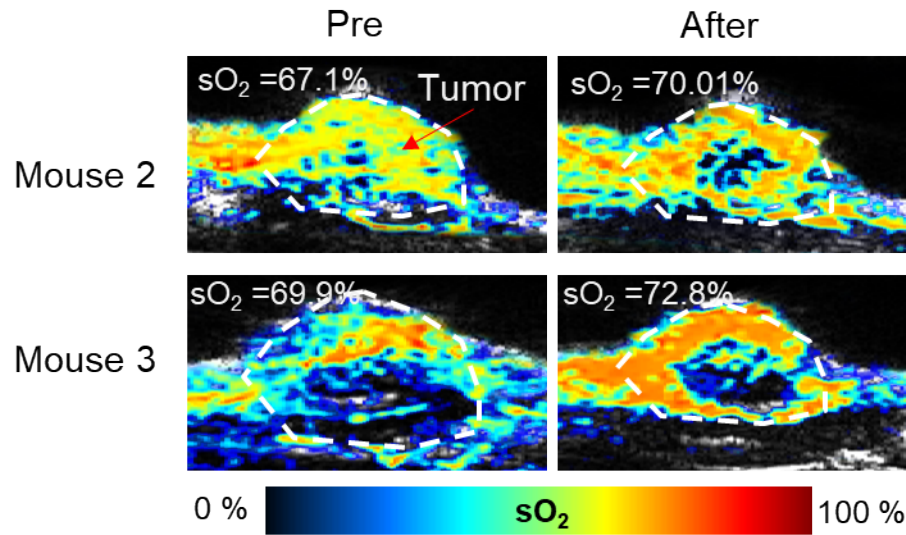


Figure S10. Representative 2D photoacoustic images of solid tumors showing parametric map of estimated oxygen saturation (sO_2) before and after treatment.

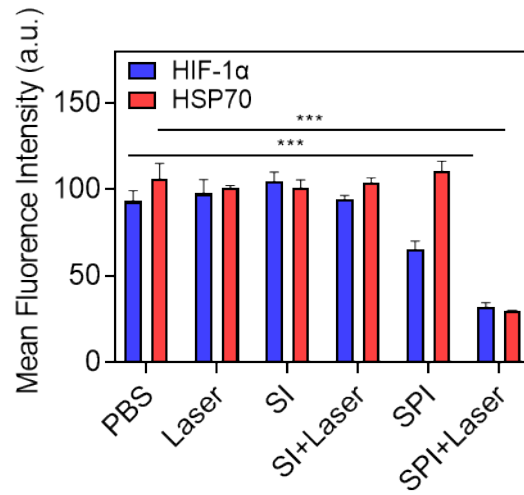


Figure S11. Quantitative fluorescence analysis of the expression of HIF-1 α and HSP70 in six different groups. The data are presented as mean \pm standard deviation (SD). The error bar is derived from triplicate measurements. *** $p < 0.001$, ** $p < 0.01$, * $p < 0.05$.

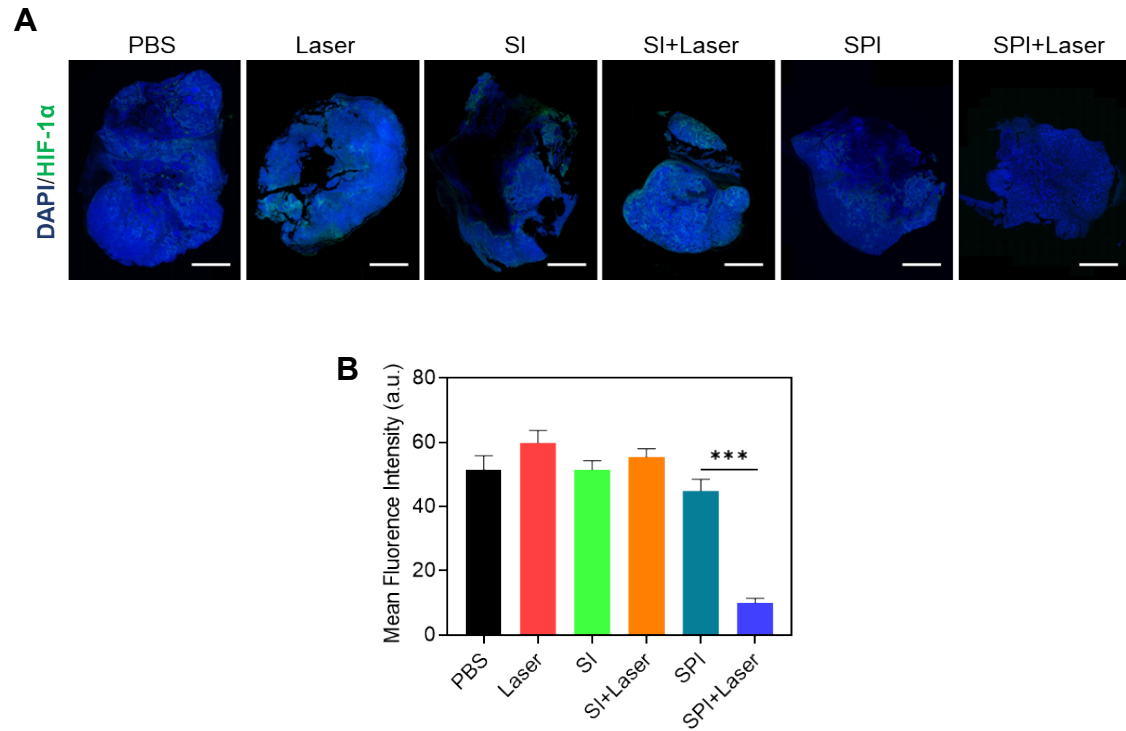


Figure S12. (A) The immunofluorescence results of the entire tumor section and (B) the quantitative fluorescence analysis of the expression of HIF-1 α . Scale bar = 2000 μ m. The data are presented as mean \pm standard deviation (SD). The error bar is derived from triplicate measurements. *** $p < 0.001$, ** $p < 0.01$, * $p < 0.05$.

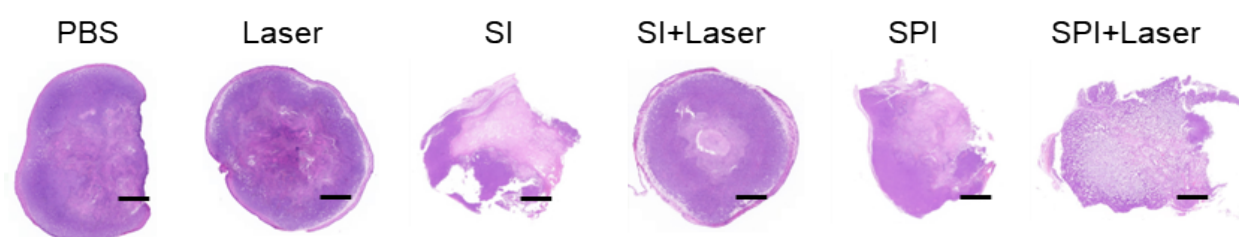


Figure S13. H&E stains of the whole tumor section from six different groups.

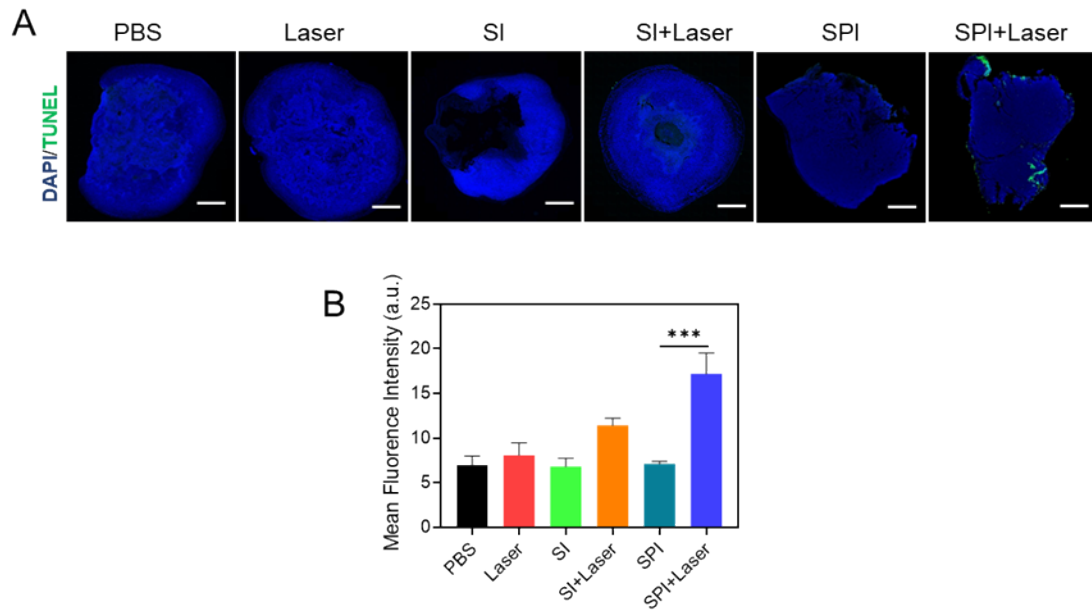


Figure S14. (A) TUNEL stains results of the entire tumor sections from six groups and (B) the quantitative analysis of mean fluorescence intensity. Scale bar = 2000 μm . The error bar is derived from triplicate measurements. *** $p < 0.001$, ** $p < 0.01$, * $p < 0.05$.

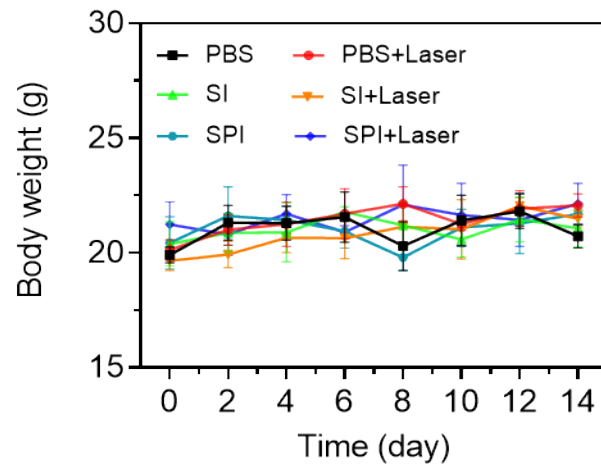


Figure S15. The changes in body weight of subcutaneous 4T1 tumor-bearing mice in different groups within 14 days.

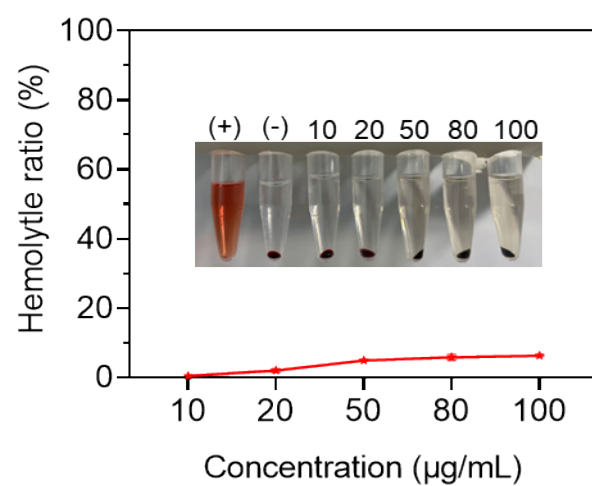


Figure S16. Hemolytic analysis of RBCs after 3 h incubation with SPI. DI water and PBS were used as the positive and negative controls, respectively.

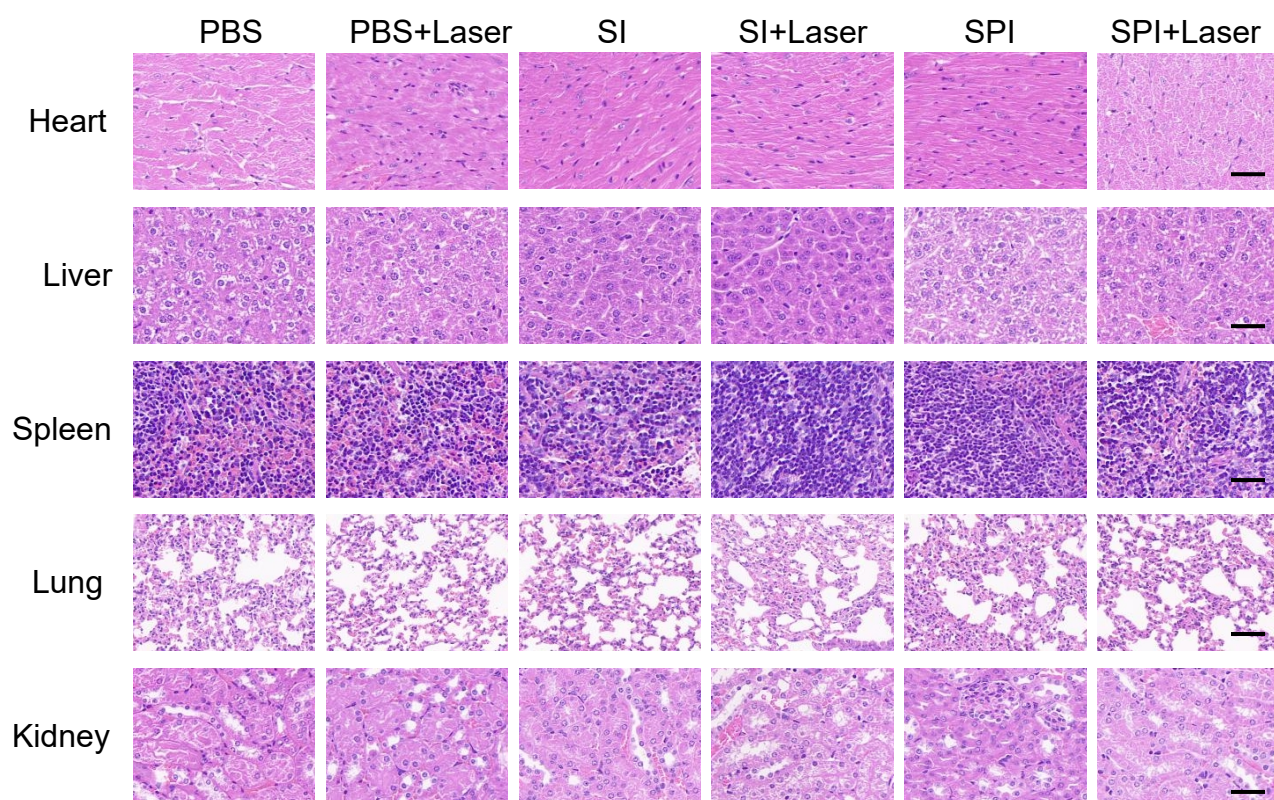


Figure S17. Hematoxylin and eosin (H&E) staining results of heart, liver, spleen, lungs, and kidneys in 6 different groups mice. Scale bars = 100 μ m.

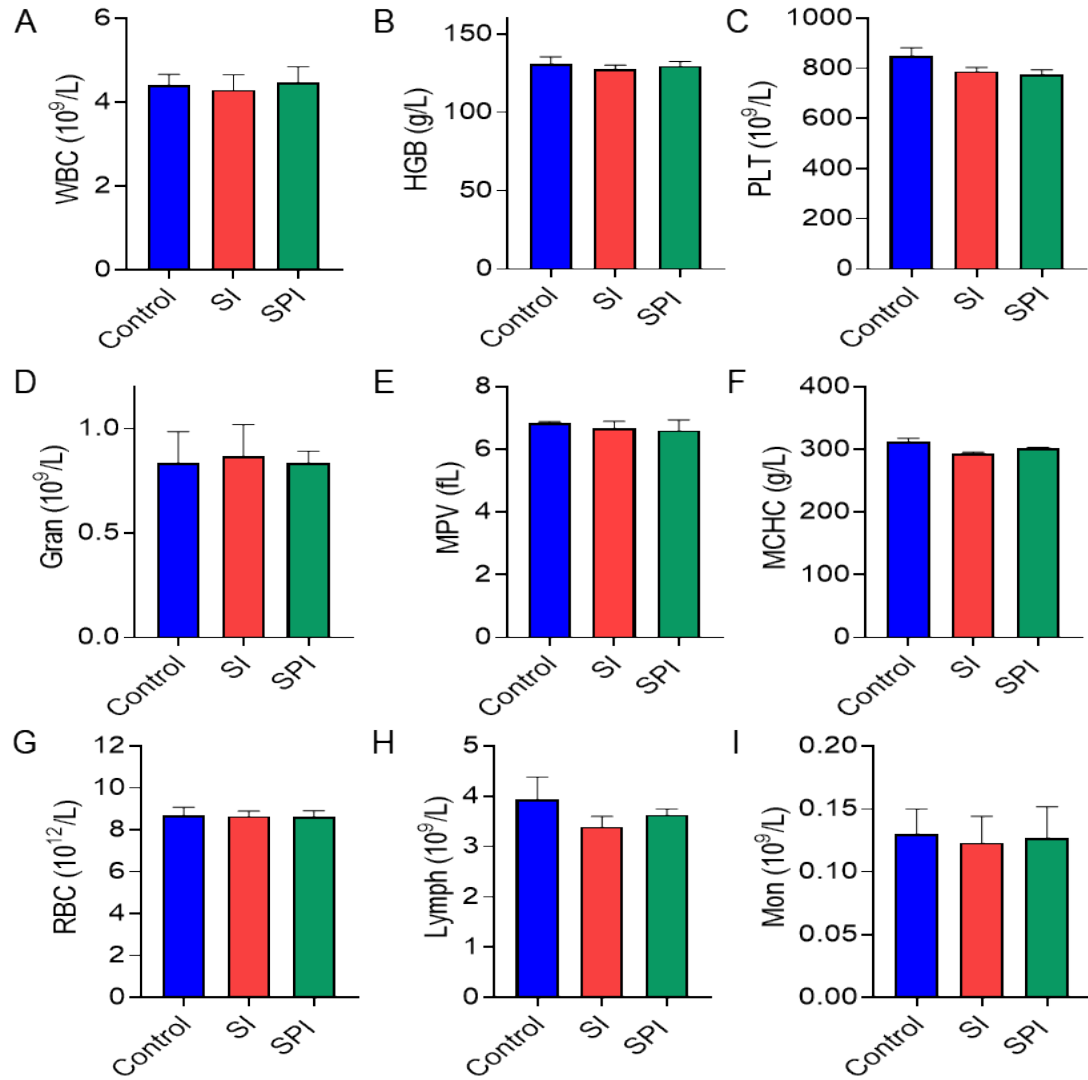


Figure S18. Blood analysis of the mice 7 days post injection of SI and SPI. (A) Number of white blood cells (WBC). (B) Hemoglobin concentration (HGB). (C) Platelets (PLT). (D) Number of neutrophilic granulocytes (Gran). (E) Mean platelet volume (MPV). (F) Mean corpuscular hemoglobin concentration (MCHC). (G) Number of red blood cells (RBC). (H) Number of lymphocytes (Lymph). (I) Number of monocytes (Mon). The data are presented as mean \pm standard deviation (SD). The error bar is derived from triplicate measurements. *** $p < 0.001$, ** $p < 0.01$, * $p < 0.05$.